Titania-PMMA nanohybrids of enhanced nanocrystallinity

**Akhmad Herman Yuwono · Junmin Xue · John Wang ·
Hendry Izaac Elim · Wei Ji**

Abstract Nanohybrid thin films consisting of titania
nanoparticles embedded in a suitable polymer matrix rep-
resent a new class of functional materials for optoelectronic
applications. For instance, our previous studies show that
titania-poly(methylmethacrylate) or TiO_2-PMMA nanohy-
brids derived from *in situ* sol-gel technique are promising
as nonlinear optical materials since they can demonstrate a
very fast recovery time of ∼1.5 picosecond and a large third-
order nonlinear susceptibility, $\chi^{(3)}$ up to 1.93×10^{-9} esu,
as observed by pump-probe and Z-scan techniques. How-
ever, it was realized that the conventional *in situ* sol-gel tech-
nique employed led to a largely amorphous TiO_2 phase in
the PMMA matrix. In order to overcome this limitation, we
have performed two modification approaches making use of
high pressure water vapor, i.e.: *pre-*and *post-hydrothermal
treatments* applied on the sol-gel precursors. The degree of
TiO_2 crystallinity in the resulting nanohybrids was studied
by XRD, FTIR, and TEM. Both approaches can enhance the
nanocrystallinity TiO_2 phase considerably and at the same
time preserve the integrity of polymer matrix. It was found,
however, that while the nanohybrid thin films derived from
the pre-hydrothermal treatment show a high absorption in
the visible length, those derived from the post-hydrothermal
treatment are highly transparent. Nonlinear optical measure-
ment using the Z-scan technique on the latter sample shows
a significant enhancement in $\chi^{(3)}$ as high as 5.27×10^{-9} esu.

1 Introduction

With the incorporation of nanosized inorganic particles into
suitable polymer matrices, nanohybrid materials are of high
interest since they can exhibit unique physical and chemical
properties, which greatly differ from those of their individ-
ual constituents [1]. In particular, nonlinear optical proper-
ties of such nanohybrids have received considerable atten-
tion for both current and future optoelectronic devices in optical
computing, real time holography, optical correlates and phase
conjugators [2]. Our previous studies have shown that titania-
poly(methylmethacrylate) or TiO_2-PMMA nanohybrids de-
rived from low temperature *in situ* sol-gel and polymerization
process are promising as nonlinear optical materials. They
exhibit nonlinear optical behavior with an ultrafast response
of about 1.5 pico second and a large third-order optical sus-
ceptibility, $\chi^{(3)}$ up to 1.93×10^{-9} esu [3, 4].

Despite the potential nonlinear properties demonstrated,
however, it is realized that the TiO_2-PMMA films, as other
titania-based polymer nanohybrids prepared by the *in situ*
sol-gel and polymerization technique are amorphous [5–7].
Brinker et al. [8] and Langlet et al. [9] suggested that the
largely amorphous nature of TiO_2-based films could be due
to the high functionality of the titanium alkoxide precursor
favoring the fast development of a stiff Ti─OH network via
condensation process. Consequently, this causes the hydrol-
ysis process taking place incompletely, which in turn hinders

A. H. Yuwono · J. Xue · J. Wang (✉)
Department of Materials Science and Engineering,
Faculty of Engineering National University of Singapore,
Block EA #07-40, 9 Engineering Drive 1, Singapore 117576
e-mail: msewangj@nus.edu.sg

H. I. Elim · W. Ji
Department of Physics, Faculty of Science, National University
of Singapore, Block S13-M01-02, 2 Science Drive 3,
Singapore 117542

the densification of TiO_2 phase. For the case of nanohybrids, such densification becomes even more difficult due to additional hindrance effect from the polymerization of organic monomers taking place concurrently. In accordance with this understanding, a previous study by Yoldas et al. [10] suggested that for synthesizing a crystalline inorganic phase directly from its alkoxide precursor, a complete hydrolysis has to occur before the condensation begins. In addition, Matsuda et al. [11] proposed that structural changes in sol-gel films can be induced by a vapor treatment in a high humidity environment at temperatures above 100°C. Further investigation by Imai et al. [12] confirmed that exposure of sol-gel derived TiO_2 films to water vapor induced rearrangement of Ti—O—Ti network leading to formation of anatase TiO_2 phase at relatively low temperature (180°C). It is therefore of interest in this work to investigate whether an appropriate water vapor treatment can induce the completion of hydrolysis process for TiO_2 sol precursor, which in turns expectedly promote the crystallization of TiO_2 phase in the resulting nanohybrids. It is also of our interest to investigate whether similar water vapor treatment can enhance the crystallinity of TiO_2 when the inorganic phase is incorporated into the nanohybrid system while at the same time it preserves the integrity of polymer matrix. Accordingly, two different approaches were performed in this work, i.e.: (i) pre-hydrothermal treatment of inorganic TiO_2 precursor, prior to the *in situ* sol-gel process, and (ii) post-hydrothermal treatment of nanohybrids derived from *in situ* sol-gel process.

2 Experimental procedures

For the first approach, a calculated amount of TiO_2 sol solution as prepared following the method described in our previous study [3] was first poured into the Teflon tube by utilizing a Teflon-lined stainless steel autoclave (Parr, Moline, Illinois). The steel autoclave was sealed carefully and furthermore heated at 80°C for various holding time from 2 to 24 h. On the other hand, the monomers, methyl methacrylate MMA and coupling agent 3-(trimethoxysilyl)propyl methacrylate)/MSMA, and initiator BPO in THF were prepared in a another reaction flask and polymerized at 60°C for 1 hour. Furthermore, the pre-hydrothermally treated sol solutions were added drop-wise over a duration of 30 min into the pre-polymerized MMA and MSMA solution, followed with rigorous stirring to form a homogeneous mixture of TiO_2-PMMA hybrid solution. The reaction was allowed to proceed at 60°C for another 2 h. In this study, the weight ratio between the inorganic and organic precursors in the reaction mixture was fixed at 60:40. In the second method, by contrast, the water vapor treatment was subjected to the nanohybrid samples derived from *in situ* sol-gel process. In detail, the autoclave containing nanohybrid samples and about 25 ml

of purified water was kept at 150°C for 24 h. A specially designed stand was placed inside this Teflon tube in order to prevent the samples from direct contact with liquid water. For comparison purposes, there were two types of samples subjected to this treatment, i.e.: nanohybrids derived from *in situ* sol-gel with and without pre-hydrothermal treatments on the inorganic precursors. Bulk samples were obtained by pouring the hybrid solutions onto a glass petri-dish, followed by drying and annealing processes. Thin film formation was realized by spin coating the solutions on quartz substrates at 3000 rpm for 20 s, prior to the same thermal treatments applied to the bulk samples.

The crystallinity in the resulting nanohybrids in this work was investigated by means of X-ray diffraction (XRD) measurements performed on Bruker AXS $\theta - 2\theta$ diffractometer using Cu K_α radiation (1.5406 Å) operated at 40 kV, 40 mA and with a step-size of 0.02° and time/step of 20 s. The corresponding infrared spectra of the samples were recorded at room temperature in the range of 4000–400 cm^{-1} using Bio-Rad FTIR model QS-300 spectrometer, which has a resolution of ± 8 cm^{-1}. The samples were further examined by using transmission electron microscopy operating at 300 keV and with a resolution of 0.14 nm (JEOL-3010). Nonlinear optical properties of the nanohybrid thin films were studied by Z-scan technique, which is a sensitive and reliable method to determine the sign and magnitude of nonlinear absorption coefficient (β) and nonlinear refractive index (n_2) [13].

3 Results and discussion

The inorganic sol solutions after pre-hydrothermal treatment at 80°C appeared translucent to opaque, depending on duration of the process which was varied from 2 to 24 h. Furthermore a preliminary XRD study was performed on pure TiO_2 powder derived from these solutions. This is particularly aimed at investigating the effectiveness of pre-hydrothermal condition in enhancing the nanocrystallinity of TiO_2 phase. Figures 1(a) and (b) show XRD traces for the TiO_2 powders thus derived, followed by drying at 60°C and 110°C, respectively. For the TiO_2 powders dried at 60°C, the treatment at 80°C for 2 to 10 hrs only provides very small increase in TiO_2 crystallinity in comparison to the amorphous structure of the sample without pre-hydrothermal treatment. They show only two weak peaks at 2θ of 25.35 and 48.25°, corresponding to (101) and (200) crystal planes for anatase TiO_2. A more considerable increase of these peaks was obtained when the treatment was performed at longer durations of 15 and 24 h. This is accompanied by the appearance of other peaks at 2θ of 38.45, 54.85 and 63.38°, corresponding to (112), (211) and (204) crystal planes. It is of interest to note that when the samples were further annealed at 110°C, a significant enhancement in intensity for all diffraction peaks has been achieved
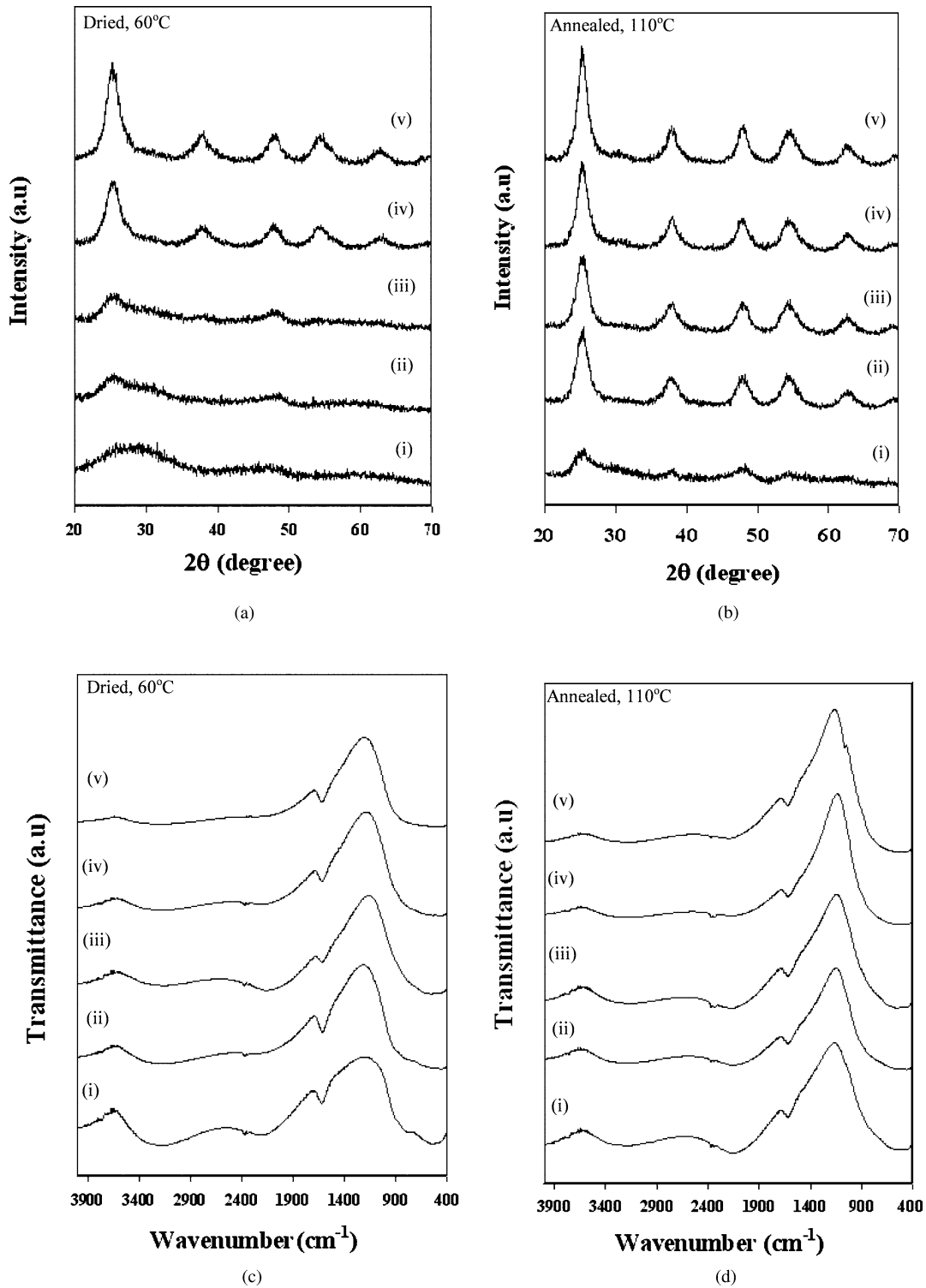
Fig. 1 (a) XRD traces of the TiO$_2$ powders dried at 60°C derived from inorganic sol solutions: (i) without and (ii, iii, iv and v) with pre-hydrothermal treatments at 80°C for 2, 10, 15 and 24 hrs, respectively; (b) XRD traces of the TiO$_2$ powder derived from the same inorganic sol solutions as (a), but annealed at 110°C; (c) and (d) the corresponding FTIR spectra of the TiO$_2$ powder for each condition showing the change in intensity for Ti—OH and Ti—O—Ti absorption bands following the trend of difference in TiO$_2$ nanocrystallinity

even for the powder derived from a short pre-hydrothermal treatment of 2 h. Longer hydrothermal treatment durations, indeed, have resulted in much more pronounced intensity for those peaks.

Figures 1(c) and (d) show the corresponding infrared (IR) absorption spectra of the samples for each condition of the hydrothermal treatments. For the TiO_2 powders dried at 60°C as shown in Fig. 1(c), the most important point to be observed is a broad absorption band at $\sim$3400–3500 cm^{-1} assigned to hydroxyl groups of Ti—OH [6]. It can be seen that the intensity of Ti—OH band in the sample without pre-hydrothermal treatment is quite intense (spectrum "(i)" in Fig. 1(c)). However, with the application of pre-hydrothermal treatment on TiO_2 sol solution prior to drying process, the intensity of this band decreases considerably. Such decrease is consistent with the increase of pre-hydrothermal treatment time (spectra "(ii)" to "(v)"). Accordingly, the absorption spectrum became almost flat when the treatment was performed for 24 hrs. By correlating these FTIR results with the difference in nanocrystallinity of TiO_2 phase shown by XRD studies, it can be confirmed that the absorption band detected at $\sim$3400–3500 cm^{-1} was that of stiff Ti—OH network resulted from too fast condensation process causing a largely amorphous nature of TiO_2 phase. Furthermore when additional driving energy was supplied from the annealing process at 110°C, the conversion from hydrolyzed titanium alkoxide product to crystalline TiO_2 took place. In general, the crystallinity promotion of TiO_2 phase upon annealing process is obviously shown by the intensity enhancement in XRD peaks given by all annealed samples (Fig. 1(b)) in comparison to those of dried ones (Fig. 1(a)). This is also demonstrated by the presence of stronger IR absorption band at 900-400 cm^{-1} provided by spectra "(i)" to "(v)" in Fig. 1(d), as compared to those of in Fig. 1(c). This band centered at $\sim$650 cm^{-1}, is accounted for by vibrations of Ti—O—Ti groups and is well-known as the characteristic peak for TiO_2 [14]. However, it is of further interest to note that while only a slight enhancement in the XRD peaks can be shown by the annealed sample derived from sol solution without pre-hydrothermal treatment (trace "(i) in Fig. 1(b)), a much more pronounced crystallinity improvement is demonstrated by those derived from pre-hydrothermal treatment with various duration of time (traces "(ii)" to "(v)"). These results, therefore, strongly confirm that such pre-hydrothermal treatment is effective in assisting the completion of hydrolysis process in the starting sol solution and preventing premature condensation to form amorphous network. It has been known that faster hydrolysis rate than condensation process can lead to the formation of order structures for TiO_2 phase [10].

Figures 2(a) and (b) are the XRD traces and FTIR spectra for the nanohybrids derived from the mixture of pre-hydrothermal treated inorganic sol solution and pre-polymerized matrix, followed by annealing at 150°C. In com-

parison to the well-established diffraction peaks shown by the annealed TiO_2 powders which were derived from treated sols for 2 to 10 h, the resulting TiO_2-PMMA nanohybrids demonstrate lower crystallinity (traces "(ii)" and "(iii)" in Fig. 2(a)). Their XRD peaks are comparable with those derived from the sol solution without pre-hydrothermal treatment (trace "(i)"). A considerable increase in intensity can only be obtained when the nanohybrids were synthesized using sol solutions pre-hydrothermally treated for 15 and 24 h (traces "(iv)" and "(v)"). In general, the crystallinities of nanohybrids here are found to be very similar to those of the TiO_2 powders dried at 60°C (Fig. 1(a)). This suggests that during mixing process with the pre-polymerized MMA and MSMA solutions, the pre-hydrothermally treated inorganic sols had been dispersed to the extent that most of the hydrolyzed titanium alkoxide was capped strongly by the organic moieties. This is realized through the role of siloxane groups of the coupling agent MSMA to provide hydrogen-bonding interactions between the acrylic groups and Ti—OH groups. This can be confirmed also with the visual appearance of the resulting nanohybrid solutions which was transparent, although the pre-hydrothermally treated precursors were translucent to opaque in appearance, strongly indicating different level of hydrolysis completion. When the annealing process was carried out, therefore, densification of the TiO_2 phase from the hydrolyzed Ti—OH groups was hindered by the formation of rigid network of polymer chains. Such condition, to some extent, was almost similar to that of the nanohybrid derived from sol solution without pre-hydrothermal treatment. This is also represented by the intensity of Ti—O—Ti absorption band, which is almost the same for all nanohybrids (Fig. 2(b)). Indeed, there was still a considerable enhancement for TiO_2 nanocrystallinity that can be observed in several nanohybrids, i.e. those were derived from the sol solution with longer pre-hydrothermal treatment (15–24 h). This could be related to the high number of TiO_2 aggregates resulted from the initial pre-hydrothermal treatment which can not be capped further by MMA and MSMA. Figure 2(c) and (d) are the TEM images showing a significant difference in TiO_2 dispersion and aggregation for the nanohybrids derived from inorganic sol solution hydrothermally treated for 2 and 24 h, respectively.

It is of further interest to apply post-hydrothermal treatment on nanohybrids derived from *in situ* sol-gel technique with and without pre-hydrothermal treatments on the inorganic precursors. For comparison purposes, post-hydrothermal treatment was performed for each type of samples at two conditions: dried at 60°C and annealed at 150°C. The XRD traces of the nanohybrids derived from these various techniques are given in Fig. 3. Firstly, it can be seen that for nanohybrids derived from pre-hydrothermal treatments at 80°C for 2 and 24 h, the intensity of their XRD peaks at both drying and annealing conditions is almost
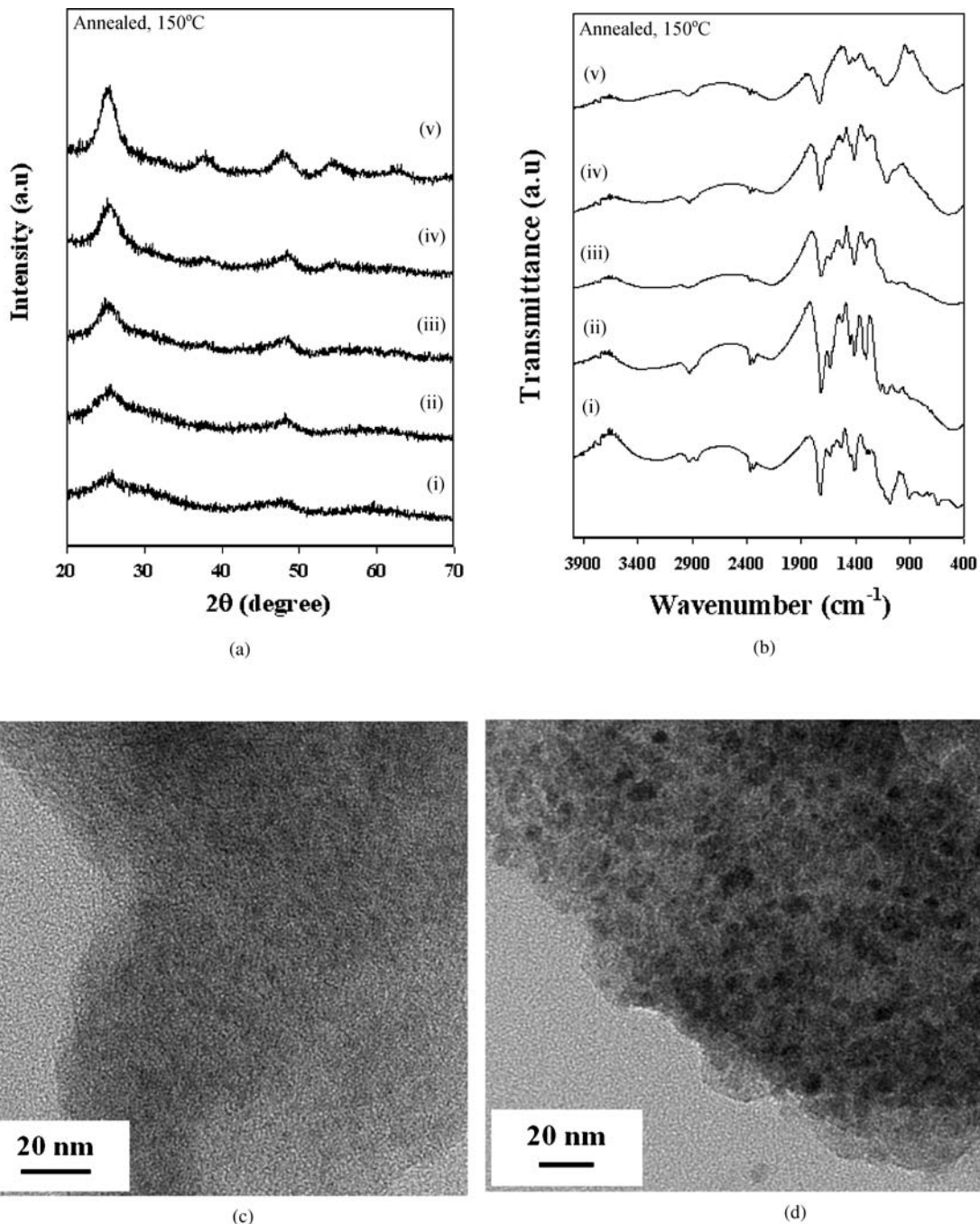
(a)

(b)

(c)

(d)

Fig. 2 (a) and (b) XRD traces and FTIR spectra of the TiO$_2$-PMMA nanohybrids annealed at 150°C for 12 hrs, which were derived from the mixture of pre-polymerized PMMA and inorganic sol solutions: (i) without and (ii, iii, iv and v) with pre-hydrothermal treatments at 80°C for 2, 10, 15 and 24 hrs, respectively. (c) and (d) TEM images of the nanohybrids derived from inorganic sol solution with pre-hydrothermal treatment at 80°C for 2 and 24 hrs, respectively

the same (traces "(i)" and "(ii)" in Figs. 3(a) and (b)). This suggests that the nanocrystallinity of TiO$_2$ phase in these nanohybrids was strongly determined by the degree of hydrolysis completion obtained from pre-hydrothermal treatment and furthermore fixed by the hindrance effect from the polymer matrix during the onset of annealing process at low temperature. In contrast, the annealed nanohybrid

which was derived from inorganic precursor without pre-hydrothermal treatment showed a slightly higher enhancement in nanocrystallinity for anatase phase (trace "(ii)" in Fig. 3(c)), as compared to the dried sample (trace "(i)"). Secondly, when the post-hydrothermal treatment was applied, all of the samples demonstrated an enhancement in their XRD peaks (traces "(iii)" and "(iv)" in Figs. 3(a)–(c)). Based on the
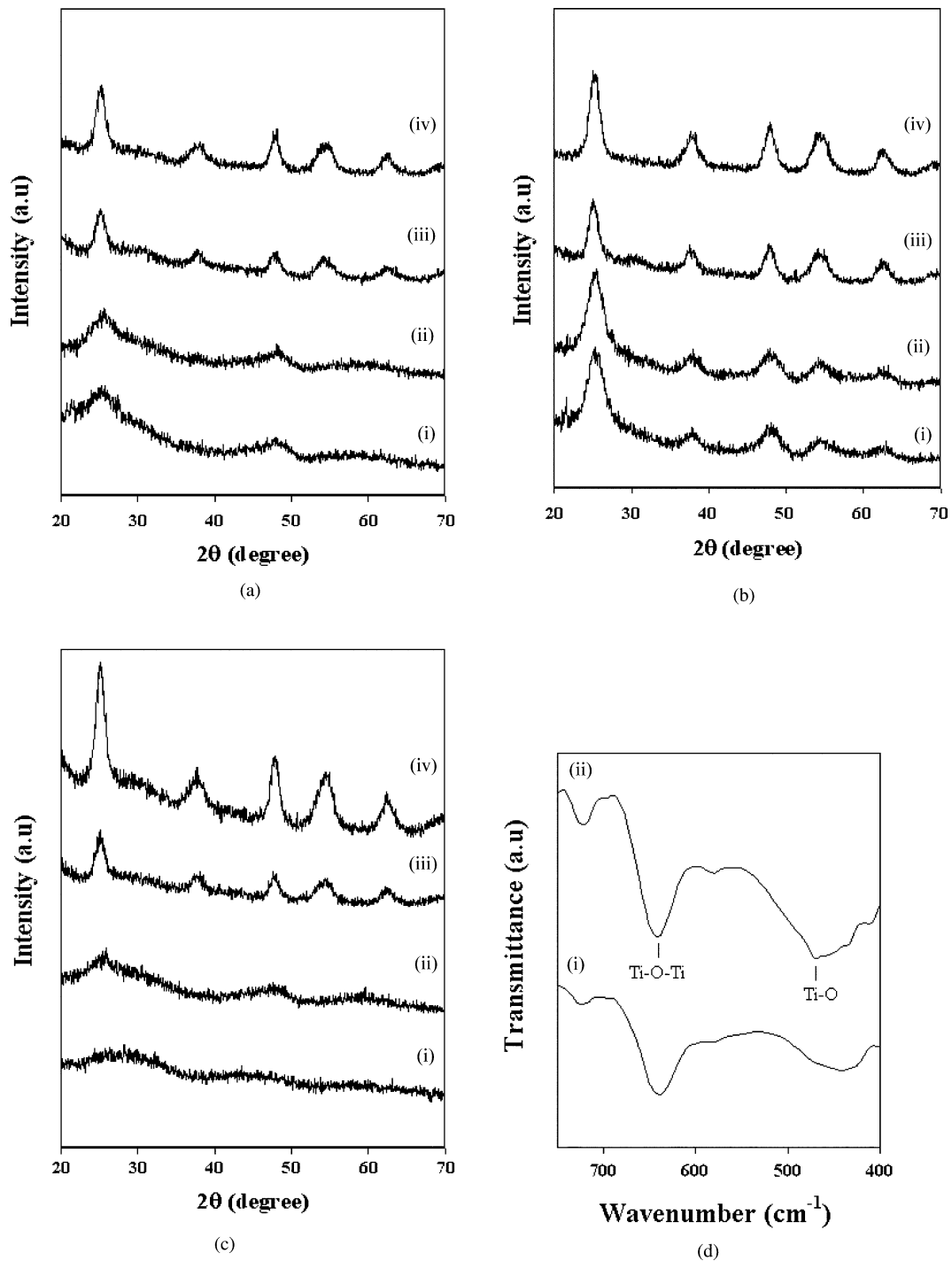
(a)

(b)

(c)

(d)

Fig. 3 XRD traces of TiO$_2$-PMMA nanohybrids: (a) with pre-hydrothermal treatment of inorganic sol solution at 80°C for 2 hrs followed by (i) drying at 60°C; (ii) annealing at 150°C for 12 hrs; (iii) and (iv) post-hydrothermal treatment at 150°C for 12 hrs after (i) and (ii); (b) with pre-hydrothermal treatment of inorganic sol solution at 80°C for 24 hrs followed by the same procedure as (a) for obtaining condition (i) to (iv); (c) without pre-hydrothermal treatment of inorganic sol solution followed by the same procedure as that of (a) and (b) to obtain condition: (i) to (iv); (d) corresponding FTIR spectra for condition (i) and (ii) in sample (c)

Imai model [12], this enhancement in crystallinity is resulted from the cleavage of strained Ti—O—Ti bonds in nanohybrids by water molecules. This results in the formation of much more flexible Ti–OH leading to the rearrangement and densi-fication of ordered Ti—O—Ti bonds and thus crystalline TiO$_2$ phase. However, such enhancement was shown to be more pronounced in the samples derived from pre-hydrothermal treatment for 2 h and without treatment, as compared to that of

with much longer treatment time (24 h). For the former, it can be concluded further that the drying and annealing processes, which were applied prior to the post-hydrothermal treatment, provided a particular effect to make further difference in the resulting TiO$_2$ nanocrystallinity. As shown by trace "(iv)" in Figs. 3(a) and (c), the XRD peaks of the samples which were annealed and post-hydrothermally treated are much sharper than that those of only dried and followed by the same post-hydrothermal treatment (trace "(iii)"). A feasible explanation for this is related to the formation of TiO$_2$ nuclei by the initial annealing process. Figure 3(d) shows the FTIR spectra of the nanohybrids which were derived from sol solution without pre-hydrothermal treatment and followed by drying at 60°C (spectrum "(i)") and by annealing at 150°C (spectrum "(ii)"), respectively. The occurrence of TiO$_2$ nuclei in these samples is represented by the stretching vibration of Ti—O bonds as a rather broad band at ~460 cm^{-1} and a small but sharp peak of Ti—O—Ti at 650 cm^{-1}. It is clearly shown that the intensity of both peaks is somewhat stronger in the annealed samples than that of the dried one, indicating the higher number of TiO$_2$ nuclei. Subsequent post-water vapor treatment thus involved these nuclei in the rearrangement of flexible Ti—O—Ti bonds. It can be understood, therefore, that the higher number of nuclei involved had led to the formation of higher number of TiO$_2$ nanocrystallites, as represented by the XRD trace "(iv)" in Fig. 3(c). It is of further interest to note that such nanocrystallinity enhancement through this mechanism is shown to be more obvious by the sample without pre-hydrothermal treatment in comparison to that of with pre-hydrothermal treatment at 80°C for 2 h. This could be related to the lesser number of nuclei in the latter since it has possessed higher number of hydrolyzed titanium alkoxide resulted from the previous pre-hydrothermal treatment with the aid of high pressure. It is likely that these hydrolyzed products are more confined in the polymer matrix than the TiO$_2$ nuclei. During the subsequent post-hydrothermal treatment, therefore, they could not contribute much to the rearrangement of flexible Ti—O—Ti bonds leading to formation of TiO$_2$ phase. This can be further confirmed by the XRD peaks of the samples derived from pre-hydrothermal treatment at 80°C for 24 h in Fig. 3(b), showing very small intensity difference between trace "(i)" and "(iii)", and also between trace "(ii)" and "(iv)". With a much higher number of fully hydrolyzed products that have been attached strongly to the polymer matrix, much less effect of post-hydrothermal treatment on these samples was observed.

Based on the above studies, it can be concluded that nanohybrid derived from inorganic sol solution without pre-hydrothermal treatment, followed by annealing and post hydrothermal treatment can provide significant crystallinity. The crystallinity is found to be comparable with that of the samples with long pre-hydrothermal treatment, followed by the same procedures. According to the UV-Vis measurement,

the transparency of the resulting films coated on the quartz substrates for the latter is rather poor. High absorption in the visible wavelength was encountered and this could be due to a great number of TiO$_2$ aggregates resulting in optical scattering. In contrast, the resulting thin film of the former nanohybrid is highly transparent. In addition, by taking other advantage from the initial annealing process applied, the integrity of polymer matrix in this nanohybrid can be well-preserved upon the involvement of water vapor. This can be seen in Fig. 4(a) showing the FTIR result of the nanohybrid (spectrum "(ii)"), in comparison to that derived from the same sol solution without pre-hydrothermally treatment, followed by annealing but without post-hydrothermal treatment (spectrum "(i)"). It is clearly shown that the intensities of C—H, C=O and C—O—C at 2950, 1737 and 1003–1258 cm^{-1} absorption bands of organic segments [5] in the post-hydrothermally treated sample were maintained and comparable to those of conventionally annealed without post-hydrothermal treatment. The FTIR result also confirms the enhanced nanocrystallinity obtained in the post-hydrothermally treated sample as has been shown previously by XRD studies. Again, this is represented by a strong absorption band in the range of 900-400 cm^{-1} with a center at ~650 cm^{-1} as the characteristic peak for nanocrystalline TiO$_2$. By contrast, the amorphous nature of the conventionally annealed sample is given by tiny peaks at ~460 and 650 cm^{-1} representing the stretching vibrations of Ti—O and Ti—O—Ti in the short-range ordered TiO$_2$ clusters. The difference in crystallinity between these two samples is further confirmed by HRTEM studies as shown in Fig. 4(b). The conventionally annealed thin film provides amorphous TiO$_2$ clusters appearing as nearly spherical nanoparticles dispersed uniformly in the PMMA matrix (image "(i)"). No clear lattice fringes can be observed from the particles. By contrast, the TiO$_2$ nanoparticles in the post-hydrothermally treated film shows well-established lattice fringe (image "(ii)"). There exists a little tendency for crystallite aggregation; however, most of the particles are still dispersed rather uniformly in the polymer matrix. The average crystallite size and standard deviation are 3.98 ± 0.97 and 9.09 ± 1.51 nm for the conventionally annealed and post-hydrothermally treated nanohybrids, respectively.

Figures 4(c) and (d) show the results of nonlinear optical measurements obtained from both nanohybrid thin films by using open and closed aperture Z-scan techniques, respectively. It is clearly shown that the nonlinear optical responses of post-hydrothermally treated sample are much larger than those of conventionally one. The absolute third-order susceptibility $\chi^{(3)}$ has been calculated from the experimental data using Sheik-Bahae's formulation [13], providing values of 1.05 × 10^{-9} and 5.27 × 10^{-9} esu for the conventionally annealed and post-hydrothermally treated nanohybrids, respectively. The value obtained by the conventionally annealed
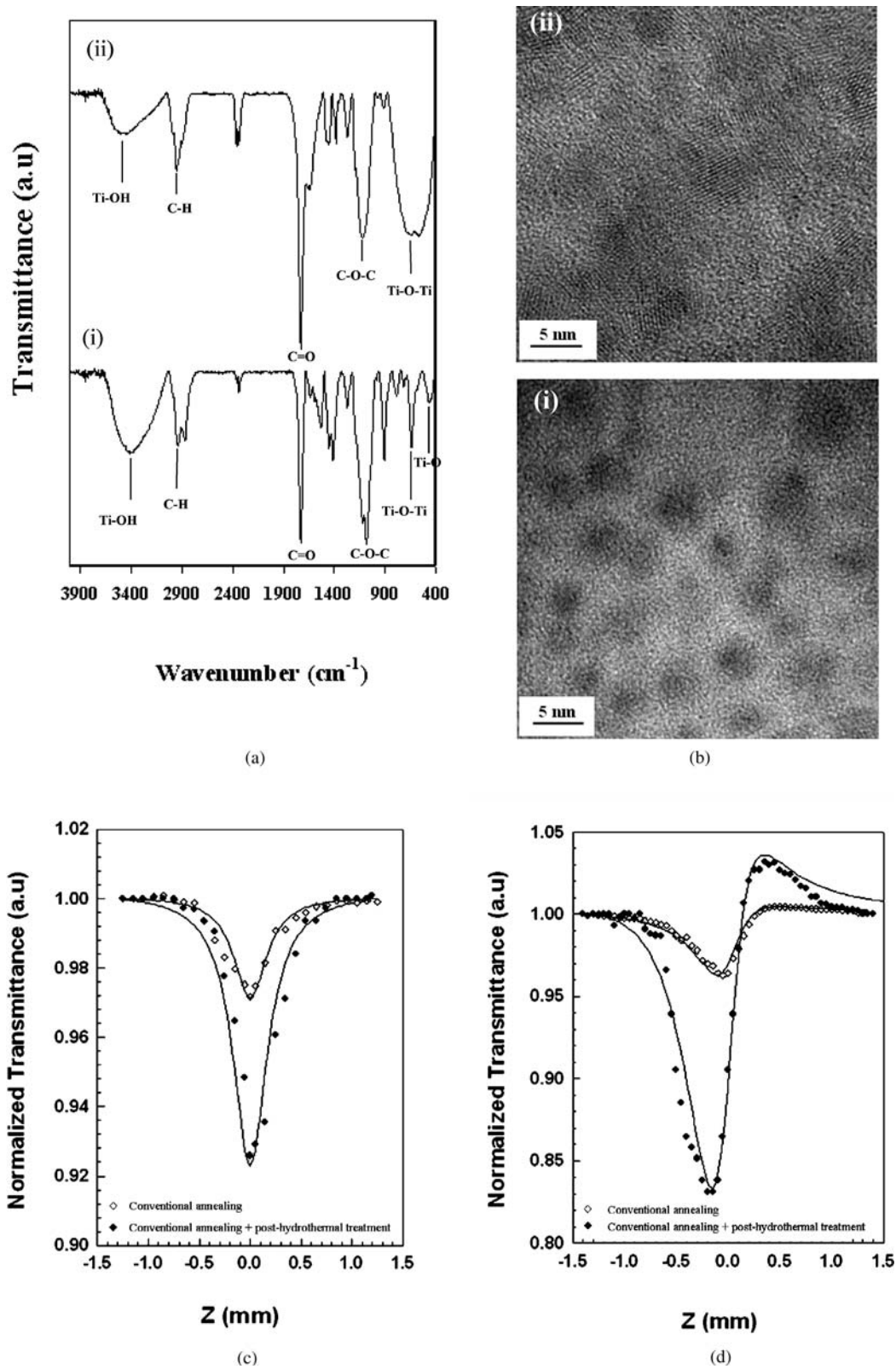
(a)

(b)

(c)

(d)

Fig. 4 (a) FTIR spectra of the TiO$_2$-PMMA nanohybrid thin films derived from inorganic sol solution without pre-hydrothermal treatment, followed by: (i) conventional annealing only; (ii) conventional anneal- ing and post-hydrothermal treatment (b) corresponding HRTEM images for thin film samples (i) and (ii); (c) and (d) open and closed Z-scan results for thin film samples (i) and (ii)

sample in the present study is comparable to that of in our previous investigation, which was 1.93×10^{-9} esu [3, 4]. This confirms a similar amorphous nature of the samples since they were prepared using the same technique. By contrast, the post-hydrothermally treated sample provides a value which is about three times larger than that can be achieved by those amorphous samples. Ai et al. [15] have proposed that nonlinear optical response in nanohybrid materials can be accounted for by the surface polarization or dielectric confinement effect resulted from the difference in refractive index between semiconductor nanoparticles and the surrounding matrix. Gan [16] has suggested that such enhancement in dielectric confinement effect of nanohybrids can be obtained by either raising the refractive index of the semiconductor or lowering the refractive index of surrounding medium (matrix). It has been reported that higher refractive index of TiO_2-based thin films can be achieved with higher crystallinity and densification of TiO_2 phase [17]. Therefore, with a much higher number of TiO_2 crystallites surrounded with well-preserved polymer matrix, it can be understood that the post-hydrothermally treated sample in this study can demonstrate a significant enhancement in third-order susceptibility $\chi^{(3)}$.

Conclusion

Two different approaches, involving hydrothermal treatment at different stages of sol-gel and *in-situ* polymerization, have been taken to enhance the nanocrystallinity of TiO_2-PMMA nanohybrids, and at the same time to maintain the integrity of the polymer matrix. Based on XRD and FTIR studies, it is shown that the pre-hydrothermal treatment on inorganic precursors is effective to assist the completion of hydrolysis process leading to formation of ordered structures for TiO_2 phase with significant crystallinity. However, the resulting nanohybrids derived from these precursors show reduced crystallinity than the pre-hydrothermally treated TiO_2 precursor. This is due to the entrapment of the pre-hydrothermally hydrolyzed segments by the organic matrix, resulting in a strong hindrance effect for the further condensation of Ti—O—Ti network. In contrast, the post-hydrothermal treatment on nanohybrid derived from inorganic sol solution without pre-hydrothermal treatment demonstrates more pronounced

crystallinity. This is resulted from the cleavage of strained Ti—O—Ti bonds in the nanohybrids by water molecules which in turn rearrange slowly and crystallize into TiO_2 nanoparticles.

A further significant enhancement in crystallinity was observed when an additional annealing at 150°C was introduced before the post-hydrothermal treatment at 150°C, in comparison to the drying at 60°C prior to the same treatment. This is related to the resultant high number of TiO_2 nuclei formed by the initial annealing process, which in turn involved in the rearrangement of flexible Ti—O—Ti bonds. HRTEM studies confirm the formation of nanocrystalline TiO_2 particles of 9.09 ± 1.51 nm in sizes. A third-order nonlinear optical susceptibility $\chi^{(3)}$ of as high as 5.27×10^{-9} esu was demonstrated by the highly transparent nanohybrid thin film with enhanced TiO_2 crystallinity and well-preserved PMMA matrix.

References

1. Y. Yang, Z.K. Zhu, J. Yin, X.Y. Wang, and Z.E. Qi, *Polymer*, **40**, 4407 (1999).
2. D.F. Eaton, *Science*, **253**, 281 (1991).
3. A.H. Yuwono, J.M. Xue, J. Wang, H.I. Elim, W. Ji, Y. Li, and T.J. White, *J. Mater. Chem.*, **13**, 1475 (2003).
4. H.I. Elim, W. Ji, A.H. Yuwono, J.M. Xue, and J. Wang, *Appl. Phys. Lett.*, **82**(16), 2691 (2003).
5. W.C. Chen, S.J. Lee, L.H. Lee, and J. L. Lin, *J. Mater. Chem.*, **9**, 2999 (1999).
6. L.H. Lee and W.C. Chen, *Chem. Mater.*, **13**, 1137 (2001).
7. C.C. Chang and W.C. Chen, *J. Polym. Sci. Part A: Polym. Chem.*, **39**, 3419 (2001).
8. C.J. Brinker and A.J. Hurd, *J. Phys. III France*, **4**, 1231 (1994).
9. M. Langlet, M. Burgos, C. Couthier, C. Jimenez, C. Morant, and M. Manso, *J. of Sol-Gel. Sci. Tech.*, **22**, 139 (2001).
10. B.E. Yoldas, *J.Mater. Sci.*, **14**, 1843 (1979).
11. A. Matsuda, Y. Kotani, T. Kogure, M. Tatsumisago, and T.Minami, *J. Am. Ceram. Soc.*, **83**(1), 229 (2000).
12. H. Imai and H. Hirashima, *J. Am. Ceram. Soc.*, **82**(9), 2301 (1999).
13. M. Sheik-Bahae, A.A. Said, T. Wei, D.J. Hagan, and E.W. Van Stryland, *IEEE J. Quantum Electr.*, **26**, 760 (1990).
14. S.X. Wang, M.T. Wang, Y.Lei, and L.D. Zhang, *J. Mater. Sci. Lett.*, **18**, 2009 (1999).
15. X.C. Ai, H. Fei, Y. Yang, L. Han, R. Nie, Y. Zhang, C. Zhao, L. Xiao, T. Li, J. Zhao, and J. Yu, *J. Lumin.*, **60/61**, 364 (1994).
16. F. Gan, *J. Sol-Gel. Sci. Tech.*, **13**, 559 (1998).
17. Z. Wang, U. Helmersson, and P.O. Käll, *Thin Sol. Films,* **405**, 50 (2002).